

Integration of Slip Detection and Grip Force Control in an Autonomous Robot Assembly Task for Space Applications

I Ishrath¹, S Barat¹, Gustavo H. Diaz², Shreya Santra², Kazuya Yoshida², Harish J. Palanthandalam-Madapusi¹

Abstract— Establishing human habitat using in-situ materials on the Moon or Mars autonomously by robotic systems is of great interest to humans. In such autonomous assembly tasks, it is crucial to integrate a slip detection capability that can detect any slipping in the grip and take corrective actions autonomously. This will enable safe handling of in-situ materials during assembly by not unnecessarily applying excessive gripping force. We construct and evaluate sliding slip detection methods (based on both heuristic and learning methods), using only the normal force recorded by a uni-axial force sensor in a robotic gripper particularly from the point of view of autonomous assembly tasks for space applications. We were able to achieve over 75% sensitivity and specificity in slip detection using LSTM (Long Short-Term Memory) based model. We also observe that training the model on simulation data alone yields very robust performance in experiments and real-time prediction, and contrary to our expectation, labeling slip in the incipient phase did not yield better performance. Further, we integrate slip detection and corrective actions with an autonomous assembly task through Robot Operating System. In an experimental demonstration of autonomous assembly task using magnetic blocks, YOLO v8 for object detection and LSTM model for slip detection, our results indicate that we are able to successfully complete with correct detection of slip and corrective actions in 9 out of the 10 demonstrations.

I. INTRODUCTION

With the renewed and significant interest in establishment of human base on the surface of Moon and Mars, there is a need to develop robotic systems for autonomous assembly of both habitat and infrastructure (such as solar panel installations). Due to the extreme nature of these environments and lack of availability of resources, autonomous robotic systems become a necessity. Among the active efforts in this direction, NASA's Johnson Space Center led development of its first humanoid robot, Valkyrie [1] explores such applications.

¹I. Ishrath, S. Barat and H. J. Palanthandalam-Madapusi are with IITGN Robotics Laboratory, Dept. of Mechanical Engineering, Indian Institute of Technology, Gandhinagar, 382424 India Email: barats@iitgn.ac.in

²G. H. Diaz, S. Santra, and K. Yoshida are with the Space Robotics Laboratory (SRL), Depart. of Aerospace Engineering, Graduate School of Engineering, Tohoku University, Sendai 980-8579, Japan.

*Corresponding author is S. Barat.

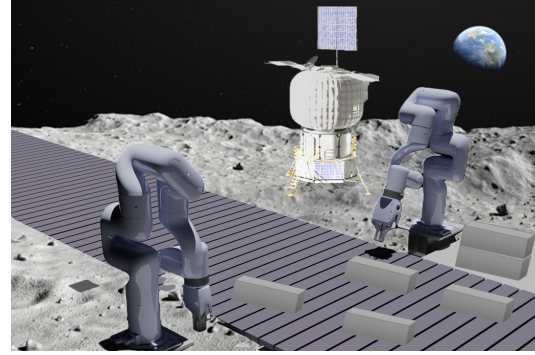


Fig. 1: An illustration of an autonomous extra-terrestrial assembly task with in-situ materials.

Zhihui et al. in [2] provide a brief analysis of the key technologies in in-space assembly, their future development trends and potential applications. Other such surveys include an earlier survey [3] by Pedersen L et al. that summarises a survey conducted by NASA and describe the state-of-the-art in space robotics.

Given the prohibitively high costs of transporting construction materials to extraterrestrial locations, one of the promising approaches that is being explored is constructing and assembling habitats using in-situ materials available on the Moon or Mars, an illustration of which is provided in Figure 1. As many of these materials may be brittle, an important functionality of any such autonomous assembly task would be to modulate the gripping force to maintain a gentle grip unless higher gripping force is needed for a task. An associated challenge with maintaining a gentle grip is that the object being held could slip from the grasp during the assembly task, and therefore leads to the requirement of slip detection and grip force modulation to avoid slip.

There has been extensive literature in the area of slip detection. Studies have explored both human slip detection mechanisms and various sensors and methods that can be used to detect slip [4]. Slip detection using tactile sensors [5], using tactile and force sensors [6], and using combination of tactile and visual information [7] have been explored. Various slip detection algorithms, including neural network based algorithms and construction of slip detection sensors have been proposed [7]–[9]. Comparative analysis of various techniques is provided in [10], discussing strengths and weaknesses in sensing

technologies. BioTac [9] and GelSight [7] sensors were among those explored for slip detection.

In this work, we focus on slip detection in an autonomous assembly task for space applications, and to take appropriate corrective action when slip is detected. For slip detection, we utilise a single-axis force sensor integrated with the gripper (to sense the gripping force) and develop methods to detect slip using variations in the gripping force only. Vision and other sensing are not utilised in the current work, and sensing slip without use of a force sensor is left for future exploration. For slip detection, we explore both heuristic methods and ML (Machine Learning)/DL (Deep Learning) methods to evaluate the performance and utility of various approaches. To explore these methods, we generate both simulation (synthetic) data from a physics-based simulation environment and experimental data from a lab test setup, and explore different variations in training and validation of the slip detection methods. We further investigate different approaches to label slip, different feature choices, and draw insights from these investigations. Finally, we incorporate the chosen slip detection method in a live laboratory demo task of autonomous assembly and demonstrate successful implementation of a real-time slip detection method along with integrating real-time corrective actions upon detection of slip.

II. TASK DESCRIPTION

We consider an autonomous assembly task in which two blocks are to be assembled together and then the assembly interacts with a third object. A lab setup with a 7-DOF manipulator arm, an RGBD eye-in-hand camera, a force sensor integrated with the gripper, two 3-D printed dummy blocks (black and blue) for assembly and a third heavy object (a pile of paper reams) to be pushed is shown in Figure 2. The manipulator in the setup is an xArm-7 (7-DOF) from UFactory equipped with a gripper, the camera utilized in the setup is the Intel Realsense D435i camera, and the force sensor used is the miniature button load cell Futek LLB350. Further, magnetic connectors are installed at the ends of the assembly blocks to simplify the mating task in the assembly, similar to the task described in [11].

The task is therefore to autonomously sense and pick up the black block from an arbitrary location and then align and assemble with the blue block and finally push the third heavy object with the assembly of the first two blocks. The grip force is to be maintained at a gentle grip level (enough for picking up and moving the objects) until a slippage in the grip is detected (most likely to occur while pushing the heavy object). In the event of slippage, the robot must autonomously adjust the grip force to maintain stability and complete the task. In the demonstration, this force adjustment is made evident by moving back by a predefined distance (8cm) and regripping with higher force. This demonstration incorporates commonly encountered scenarios in space

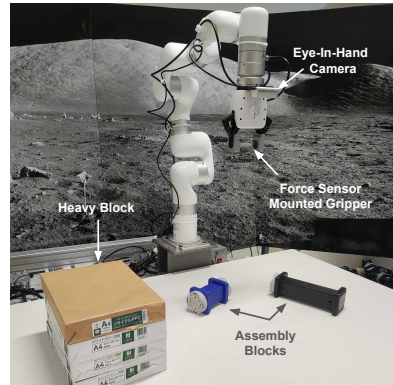


Fig. 2: Lab Demo Task: Lab setup demonstrating the assembly task, showcasing blue and black assembly blocks with magnetic connectors, a heavy block made of a stack of reams of paper, and the robot equipped with an eye-in-hand camera and fingertip force sensor mounted gripper.

assembly operations and effectively showcases object detection, slip detection, autonomous corrective action, and autonomous assembly capabilities. We next describe the slip detection methodology including generation of simulation and experimental data.

III. SLIP DETECTION

A robotic gripper can experience sliding, rolling, and tipping slips. We focus our attention on sliding slip, which manifests as a linear relative movement between the gripper and the object. Among the several approaches available, we choose the approach of analyzing normal force due to its seamless integration into our experimental setup. While there have been studies on what features are likely to be observed in the force sensor during slip (for example, presence of a steep gradient in the sensed normal force during initiation of slip [5], [6], [9]), given the high stochasticity and variability in the magnitude and nature of the features with various grip forces, friction coefficients, and other factors, we explore both heuristic and learning-based methods. We discuss the dataset generation methodology, slip tagging process, training and testing regime in further sections.

A. Dataset generation

With a focus on sliding slip, we generate simulation (synthetic) and experimental data as described below.

1) *Simulation (Synthetic) Dataset:* We employed CoppeliaSIM (Bullet 2.78) as a physics engine to generate the necessary data. Figure 3a illustrates the simulation environment in which a motor generates normal force, and a prismatic block is manipulated to simulate sliding slip. Key variables such as normal force and coefficient of friction were systematically varied to ensure a diverse dataset. Normal force ranged from 0.02N to 5.0N in 150 steps, while the coefficient of friction (μ) ranged from 0.2 to 0.8 in 20 steps. Hence, 3000 different cases were generated and corresponding forces were recorded using force sensor. Data sampling rate was set at 20 Hz.



(a) Simulation Setup

(b) Experimental Setup

Fig. 3: Simulation and Experimental Setup for data collection of sliding slip for a range of grasping forces.

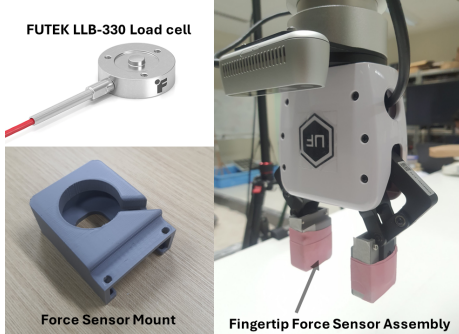


Fig. 4: Integration of Force Sensor with X-Arm Gripper: Futek LLB-330 force sensor is affixed to the fingertip using a custom-designed mount, with a rubber coating to enhance gripping during manipulation.

2) *Experimental Dataset:* Similar to the simulation setup, data for sliding scenario was gathered by fixing the 3-D printed assembly block by clamping it to the table (using a C clamp) and commanding a motion to the robot while it is grasping the block, as illustrated in Figs. 3b and 4. Since the gripper does not have force-control capability, the gripping force was modulated by controlling the position command of the gripper (tighter closing position command while holding an object produced larger gripping force as was verified by force sensor readings). Four such gripping forces were used and the force sensor readings were recorded for 100 instances of sliding slip. The data acquisition frequency was 250Hz, which was down-sampled to 20Hz for further processing.

B. Slip Labeling

Labeling slip is crucial for testing/training various methods and algorithms (particularly supervised machine learning models). We adopted two approaches to label slip instances. The first approach focused on incipient slip, which identifies and labels the starting phase of slip when the object begins to slip. In the second approach, we tagged slip occurrences whenever there was relative motion between the object and the gripper. This approach is referred to as relative motion slip in subsequent discussions. Figure 5 illustrates the tagging for a sample dataset. It is expected that signatures of slip will likely be clearest at the incipient phase, nevertheless, we intended to test and compare both these approaches.

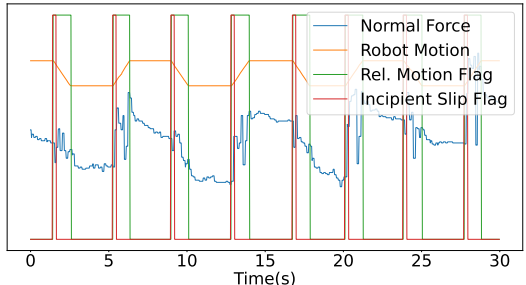


Fig. 5: Incipient slip and Relative motion slip labeling on sample experimental normal force data - A short period when the slip initiates is labeled as incipient slip while the entire period of relative motion between the gripper and the object is labelled as Relative motion slip.

C. Heuristic Model

Simple threshold based criteria on the gradient of the normal force was chosen as a potential classifier of slip. This was based on the understanding from the literature that a steep gradient in the normal force is to be expected at the instance of slip. This choice was made after comparing with about half a dozen criteria inspired from slip literature [6], [9]. Further, based on heuristic tuning, the maximum gradient in the force was computed in a stretch of data with no slip, and then a threshold of 3 times of that maximum gradient of the force was chosen as an indicator of slip. This heuristic criteria was developed based on experimental data and is used for further comparison with Machine learning models.

D. Machine Learning Models

Utilizing both the synthetic data set (much larger with wider variations) and the experimental dataset (smaller), we explored multiple well-known architectures in the literature for binary classification of time-series data. These included basic RNN (Recurrent Neural Networks), CNN (Convolutional Neural Network), SVM (Support Vector Machine), Random Forest, and LSTM (Long Short-Term Memory). In all model training, unless otherwise mentioned, only 70% of the data was utilized while 30% was retained for testing. Cross-entropy was chosen as the loss function and the default Xavier normal weight initializer was used.

E. Analysis and Discussion

The results of using the heuristic model on both the simulation dataset and the experimental dataset are summarised in Table I. Figure 6a shows the comparison of true slip and the predicted slip using the heuristic model with the simulated data and Figure 6b on the other hand shows how the slip is detected on experimental data using the same algorithm. It is clear that heuristic model has a low sensitivity in both simulation data and experimental data. In other words, the occurrence of false negatives is high in this approach.

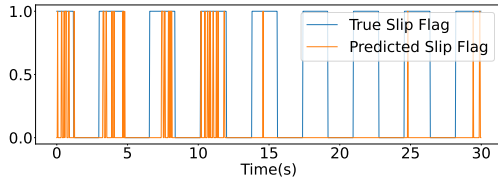
Table II summarizes the results obtained from training each architecture individually on simulation and

TABLE I: Performance metrics of Heuristic Model

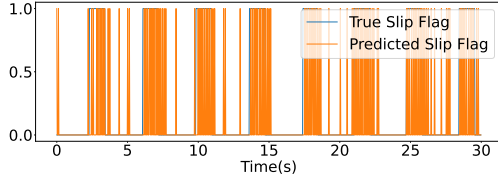
| Input | Labeling Approach | Specificity (Simulation Data) | Sensitivity (Simulation Data) | Specificity (Experimental Data) | Sensitivity (Experimental Data) |
|----------------|-------------------|-------------------------------|-------------------------------|---------------------------------|---------------------------------|
| Gradient Force | Rel. motion | 95.88 | 28.09 | 86.82 | 24.17 |

TABLE II: Performance Metrics of Various Machine Learning Algorithms Trained on Simulation and Experimental Data

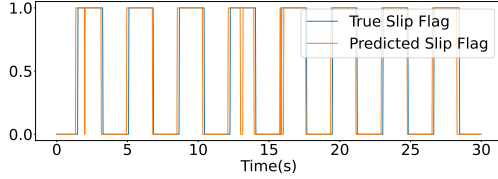
| Models | Model Trained on | Sensitivity (Simulation Data) | Specificity (Simulation Data) | Sensitivity (Experimental Data) | Specificity (Experimental Data) |
|---------------|-------------------|-------------------------------|-------------------------------|---------------------------------|---------------------------------|
| Basic RNN | Simulation data | 100 | 100 | 93.7 | 19.3 |
| | Experimental data | 88.74 | 3.68 | 80.66 | 63.6 |
| CNN | Simulation data | 85.4 | 84.4 | 100 | 0 |
| | Experimental data | 93.3 | 10.2 | 43.1 | 63.4 |
| SVM | Experimental data | 83.5 | 84.7 | 78.8 | 92.4 |
| | Simulation data | 86.3 | 83.7 | 72.31 | 91.5 |
| Random Forest | Experimental data | 62.8 | 87.1 | 92.1 | 98.9 |
| | Simulation data | 95.2 | 96.1 | 78 | 93.1 |
| LSTM | Simulation data | 76 | 52 | 74 | 97 |



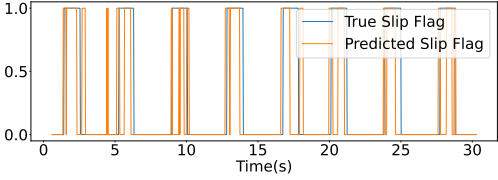
(a) Simulated Data using Heuristic Model



(b) Experimental Data using Heuristic Model



(c) Simulated Data using LSTM Model



(d) Experimental Data using LSTM Model

Fig. 6: True vs Predicted Slip using the Heuristic and LSTM models

experimental data, showcasing sensitivity and specificity metrics. While the results in Table II could be further improved through hyperparameter tuning for each model, our primary objective was to evaluate and compare various models and select one for further analysis. "Sensitivity" is defined as the ratio of true positives (Slip flag is True) to total number of positives, while

"Specificity" defined as the ratio of true negatives (Slip flag is false) to total number of negatives was used for performance analysis. It is observed that generally models trained on simulation data tend to perform in terms of sensitivity and specificity for both the rest of the simulation data (30 % that was not used in training) and the experimental data. Initial observations indicated that algorithms like linear SVM and Random Forest exhibited promising performance when tested on experimental data, particularly beneficial for handling real sensors with noisy data. However, to further explore variations in slip labeling approaches and input types such as raw data, normalized data, gradients, or normalized gradients, we opted for LSTM, a well-established deep learning architecture suited for such applications.

The LSTM based model (1 LSTM layer with 50 neurons, 1 hidden layer with 100 neurons and 1 output layer with single neuron) was trained separately on simulation dataset and experimental dataset with further variations in input to the network and criteria for labeling slip.

a) *Inputs to the Network:* Four different options for inputs to the network - Force, Normalized Force, Gradient of Force and Normalized Gradient, are considered. Furthermore, three different batch tagging strategies are considered. In these batch tagging strategies, a sliding batch (window) of 20 normal force samples are considered and the following criteria applied on the batch:

1. Rel. motion slip (10) - If at least 10 of the 20 samples have positive slip flag as per the relative motion labeling approach, the batch is considered to have a slip tag.
2. Rel. motion (5) - If at least 5 out of the 20 samples have positive slip flag as per the relative motion labeling approach, the batch is considered to have a slip tag.
3. Incipient (2) - If at least 2 incipient slip flags are present in the batch of 20, the batch is considered to be a slip condition.

Based on the above variations, Table III show the obtained performance metrics for 12 representative com-

binations when the model was trained using 70% of the simulation data (with the remaining 30 % used for testing). The performance of the model when trained on experimental data was poorer and the results are not included here in the interest of space. The predicted slip and the true slip using the LSTM based model trained on simulation data and based on 1st tagging criteria with normal force as input is presented in Figure 6c and 6d on sample simulation and experimental data.

From Table III we see that performance of models trained on simulation data continue to perform better both on the remaining simulation data and experimental data. Out of the various combinations of input and slip labeling possible, based on the sensitivity and specificity scores on both simulated and experimental data set, we see that Model 2, that takes force as input and categorises slip when at least 5 slip flags are found and Model 8, that takes Gradient of Normalised force as input and categorises slip when at least 5 slip flags perform the best. However, based on simplicity and convenience in data preparation and processing, for the real-time implementation, we chose Model 1, that has comparable performance but has a higher threshold to categorise slip (count of at least 10 slip flags in a batch of 20).

IV. EXPERIMENTAL INTEGRATION AND DEMO TASK

The force sensing, slip detection algorithm, vision system, manipulator and gripper control, gripper force control, and the overall assembly task specifications (and corrective actions in case of slip) were integrated within Robot Operating System (ROS) environment as depicted in Figure 8.

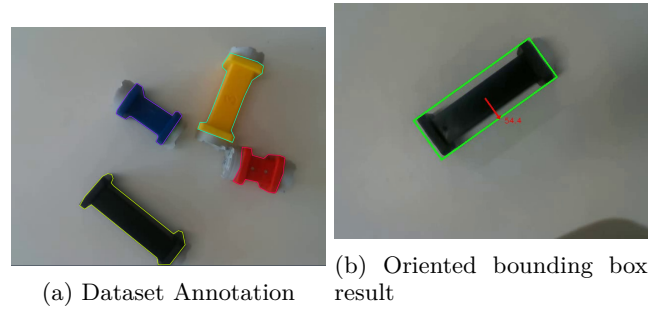


Fig. 7: Annotation and Results of Object Detection Dataset: (a) Labeling using Roboflow. (b) Results depicting the orientation angle of the long side of the object with horizontal.

TABLE III: Performance metrics of LSTM model (Trained on Simulation Dataset) with variations in input data and tagging

| Model Sr.No | Input | Labeling Approach | Specificity (Simulation Data) | Sensitivity (Simulation Data) | Specificity (Experimental Data) | Sensitivity (Experimental Data) |
|-------------|---------------------------|-------------------|-------------------------------|-------------------------------|---------------------------------|---------------------------------|
| 1 | Force | Rel. motion (10) | 96.1 | 95.2 | 93.1 | 78 |
| 2 | Force | Rel. motion (5) | 98 | 98 | 92.1 | 83 |
| 3 | Force | Incipient (2) | 81 | 86 | 81 | 3.9 |
| 4 | Normalized Force | Rel. motion (10) | 97.2 | 94.1 | 49 | 18 |
| 5 | Normalized Force | Rel. motion (5) | 97 | 97 | 37 | 26 |
| 6 | Normalized Force | Incipient (2) | 82 | 85 | 82 | 3.8 |
| 7 | Force Gradient | Rel. motion (10) | 86 | 88 | 67 | 6.6 |
| 8 | Force Gradient | Rel. motion (5) | 83 | 91 | 34 | 13 |
| 9 | Force Gradient | Incipient (2) | 83 | 76 | 81 | 5 |
| 10 | Normalized Force Gradient | Rel. motion (10) | 96 | 89 | 85 | 79 |
| 11 | Force Gradient | Rel. motion (5) | 96 | 92 | 82 | 94 |
| 12 | Force Gradient | Incipient (2) | 82 | 73 | 83 | 21 |

For detecting the position and orientation of the assembly blocks, YOLO v8 Oriented Bounding Box (OBB) model [12] is employed. A dataset was created by extracting frames from a video capturing scenarios with four different colored assembly blocks arranged in various configurations and orientations. These datasets were labelled to train the OBB model using Roboflow [13] (results illustrated in Figure 7).

The integration block acts as the master code, receiving inputs about assembly blocks positions and orientations and slip flags. It incorporates assembly logic discussed in Section II. To mitigate the risk of false positives, an additional slip flag aggregator (verification) layer is implemented within the integration code. Here, the latest ten slip flags are collected, and the slip is declared only if more than six flags indicate slippage.

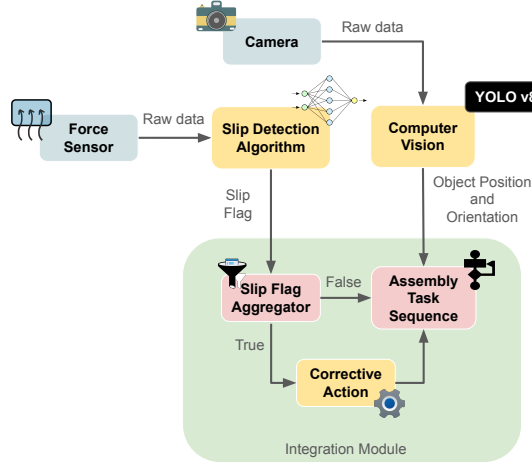


Fig. 8: Illustration of the overall integration process within ROS: The computer vision module provides object pose information, while the slip detection module predicts and publishes slip flags based on force sensor signals. Additionally, a slip flag aggregator helps mitigate issues with isolated instances of false positives and negatives.)

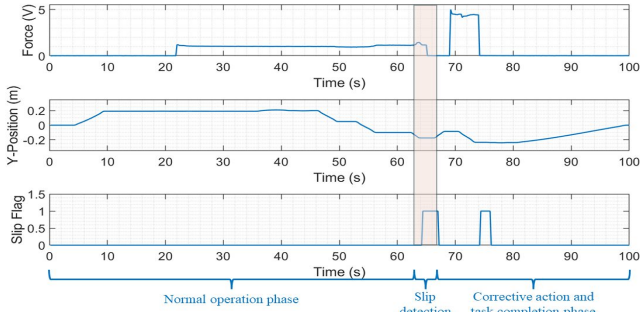


Fig. 9: Experimental Results: Data on Force, Y-coordinate of the robot, and slip Flag. The autonomous assembly task progression is segmented into three phases: Normal Operation, Slip Detection, Corrective Action, and Task Completion

This approach helps address issues related to isolated instances of false positives and false negatives.

The UFactory gripper, being position-controlled, lacks contact force control capabilities. Hence, the gripping force was modulated by controlling the position command of the gripper (tighter closing command produces a larger gripping force when an object is being held as was verified through the force sensor readings).

A. Results and Discussion

Figure 9 provides data from one complete demonstration of the assembly task that was successfully completed, and shows normal gripping force, Y-coordinates of the robot, and the final slip flags following the additional slip aggregator (verification) layer. The motion (Y-position plot) in the first 10 second corresponds to

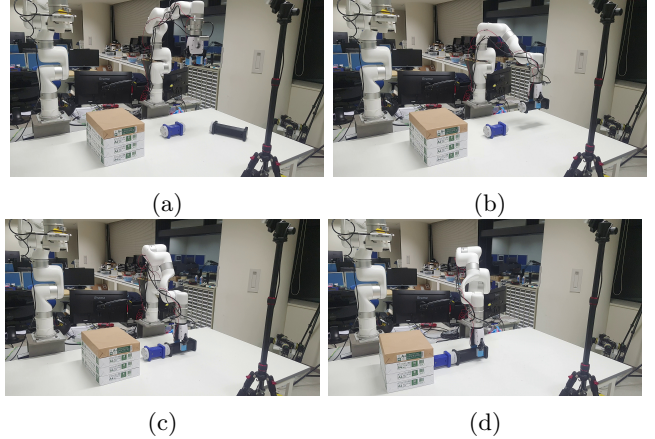


Fig. 10: Experimental Progression: (a) Robot analyzes the position and orientation of randomly placed assembly blocks. (b) Autonomously picks up the black block. (c) Joins two assembly blocks with magnetic connector. (d) Attempts to push heavy block resulting in slip. The robot responds by holding the black block with higher force and successfully completes the task.

the robot picking up the black block autonomously (after detecting the blocks and their orientations), and the two sections of motion from about the 46-second mark to the 56-second mark is first assembling the black block with the blue block, and the second motion to bring the assembly in contact with the third heavy object. This entire sequence of operations is labeled as normal operation phase as there is no slipping in this phase. However, when the robot attempts to push the third heavy block with the assembly of the first two blocks, there is a slip in the grip that is successfully detected (as seen in the slip flag plot in the highlighted region). Upon successful detection of the slip, the robot takes corrective action by releasing the grip, and executing a small backward motion of (8cm) (seen around the 66-second mark), re-grasping with a tighter grip (as seen in the normal force plot just before the 70-second mark) and then completing the task.

It is noted that around the 74-second mark, the force signal exhibits a sharp decline from a high force value to zero when the grip is released and the slip detection model produces false positives. This aspect requires refinement in future work to ensure that the grasp and release processes are not erroneously classified as slip events. We further report that in a sequence of 10 tests of the complete autonomous assembly and pushing demo task, it was observed that the integrated algorithm was able to perform the task successfully (including successful detection of slip and successful corrective action) on 9 occasions out of 10. On one occasion, the algorithm failed to detect slip correctly. Snapshots from a successful task completion is shown in Figure 10.

V. CONCLUSIONS

We constructed and evaluated both heuristic and ML/DL based slip detection models for an autonomously assembly task for space applications. While heuristic models are simple, they failed to produce performance suitable for real-time operations within the assembly task. Out of the ML/DL methods explored, the LSTM model was used due to ease of integration, acceptable performance and wide range of applications. While both simulation data and experimental data were generated, interestingly, the models trained on simulation data performed better in predicting slip in both simulations and experiments (possibly due to the higher quantity of data and the rich variety of cases captured in the simulation data). Training using a mix of experimental and simulated data remains to be explored in future work. Furthermore, while incipient slip labeling was expected to be a better approach, results demonstrated relative motion based tagging yields more robust results. Finally an autonomous assembly task incorporating camera-based block pose detection of assembly blocks, along with the slip detection model, with corrective actions upon detection of slip, was implemented through ROS. In a sequence of 10 autonomous assembly tasks, 9 out of 10 cases were successful including successful detection of slip and autonomous corrective actions.

VI. ACKNOWLEDGEMENT

This work was supported by the JST Sakura Science Exchange Program 2023-24. The authors would like to thank Luca Nunziante for the extensive assistance in the setup of the experiments.

REFERENCES

- [1] N. A. Radford, P. Strawser, K. Hambuchen, J. S. Mehling, W. K. Verdeyen, A. S. Donnan, J. Holley, J. Sanchez, V. Nguyen, L. Bridgwater et al., “Valkyrie: Nasa’s first bipedal humanoid robot,” *Journal of Field Robotics*, vol. 32, no. 3, pp. 397–419, 2015.
- [2] X. Zhihui, L. Jinguo, W. Chenchen, and T. Yuchuang, “Review of in-space assembly technologies,” *Chinese Journal of Aeronautics*, vol. 34, no. 11, pp. 21–47, 2021.
- [3] L. Pedersen, D. Kortenkamp, D. Wettergreen, and I. Nourbakhsh, “A survey of space robotics,” in *Proceeding of the 7th International Symposium on Artificial Intelligence, Robotics and Automation in Space*, no. AM-11. European Space Agency, 2003.
- [4] M. T. Francomano, D. Accoto, and E. Guglielmelli, “Artificial sense of slip—a review,” *IEEE Sensors Journal*, vol. 13, no. 7, pp. 2489–2498, 2013.
- [5] E. Holweg, H. Hoeve, W. Jongkind, L. Marconi, C. Melchiorri, and C. Bonivento, “Slip detection by tactile sensors: algorithms and experimental results,” in *Proceedings of IEEE International Conference on Robotics and Automation*, vol. 4. IEEE, 1996, pp. 3234–3239.
- [6] C. Melchiorri, “Slip detection and control using tactile and force sensors,” *IEEE/ASME transactions on mechatronics*, vol. 5, no. 3, pp. 235–243, 2000.
- [7] J. Li, S. Dong, and E. Adelson, “Slip detection with combined tactile and visual information,” in *2018 IEEE International Conference on Robotics and Automation (ICRA)*. IEEE, 2018, pp. 7772–7777.
- [8] M. Stachowsky, T. Hummel, M. Moussa, and H. A. Abdulla, “A slip detection and correction strategy for precision robot grasping,” *IEEE/ASME Transactions on Mechatronics*, vol. 21, no. 5, pp. 2214–2226, 2016.
- [9] Z. Su, K. Hausman, Y. Chebotar, A. Molchanov, G. E. Loeb, G. S. Sukhatme, and S. Schaal, “Force estimation and slip detection/classification for grip control using a biomimetic tactile sensor,” in *2015 IEEE-RAS 15th International Conference on Humanoid Robots (Humanoids)*, 2015, pp. 297–303.
- [10] R. A. Romeo and L. Zollo, “Methods and sensors for slip detection in robotics: A survey,” *Ieee Access*, vol. 8, pp. 73 027–73 050, 2020.
- [11] C. Boucher, G. H. Diaz, S. Santra, K. Uno, and K. Yoshida, “Integration of vision-based object detection and grasping for articulated manipulator in lunar conditions,” in *2024 IEEE/SICE International Symposium on System Integration (SII)*, 2024, pp. 484–489.
- [12] G. Jocher, A. Chaurasia, and J. Qiu, “Ultralytics yolov8,” 2023. [Online]. Available: <https://github.com/ultralytics/ultralytics>
- [13] B. Dwyer, J. Nelson, T. Hansen, and et. al., “Roboflow (version 1.0),” 2024. [Online]. Available: <https://roboflow.com/>